Evaluation of weak interface effect on the residual stresses in layered SiC/TiC composites by the finite element method and x-ray diffraction

Shuyi Qin, Dongliang Jiang, and Jingxian Zhang
The State Key Laboratory of High Performance Ceramics and Superfine Microstructure, Shanghai Institute of Ceramics, Chinese Academy of Sciences, 1295 Ding Xi Road, Shanghai 200050, People's Republic of China

Jining Qin
State Key Laboratory of Metal Matrix Composites, Shanghai Jiao Tong University, 1954 Hua Shan Road, Shanghai 200030, People's Republic of China

(Received 14 May 2001; accepted 18 February 2002)

A symmetrically layered SiC/TiC ceramic with a gradual structure was designed by the finite element method (FEM). After sintering, proper thermal residual stress was introduced into the ceramic due to the coefficients of thermal expansion mismatch between the different layers. After different SiC + C interlayers were inserted into the layers to weaken the interface, the effect of the composition of the SiC + C interlayers between the layers on the residual stress was evaluated. It was found that the weak SiC + C interlayer had little relaxation effect on the residual stress distribution. These ceramics were then fabricated by aqueous tape casting, stacking, and hot-press sintering. An x-ray stress analyzer was used to test the surface stress conditions of the sintered materials. The tested surface stress of the layered SiC/TiC ceramic without interlayer was very close to the FEM calculation. However, there were differences between the tested and calculated results of the layered SiC/TiC ceramics with interlayers; the reason for this was analyzed.

I. INTRODUCTION

In the past decade, layered ceramics have been studied extensively because they can show dramatically improved strength, fracture toughness, and damage and fatigue resistance compared with monolithic ceramics.[1–6] Layered ceramics can be divided into two categories. One is surface-compression-strengthened layered ceramics with strong interface bonding, such as the ZrO_2/Al_2O_3 system.[7,8] The other is laminated ceramics with weak interface bonding, such as SiC/C and Si_3N_4/BN systems.[9–11] The former is strengthened or toughened by the introduction of surface compressive stress due to coefficient of thermal expansion (CTE) mismatch between different layers. The latter is toughened by crack propagation along the weak interface between layers. If both the above strengthening and toughening mechanisms could synergetically work together, such a ceramic body could possibly show even better properties. However, few studies have been done along this approach.

It is evident that when a pure bending load is applied to a structure with a rectangular cross section, the stress condition varies linearly from maximum tension on the surface to zero stress on the central plane.[12] Thus, we believe that thermal residual stress in a symmetrically layered ceramic should be designed to vary gradually from surface compressive stress to inner tensile stress. Therefore, such a structure should have gradual compositions from the surface to the center. In such a case, the finite element method (FEM) is proper for designing the structure because FEM is a powerful tool for calculating residual stress distribution in composites.[13,14] Furthermore, FEM is also suitable for evaluating the effect of imperfect interlaminar interface on the mechanical properties of laminated composites.[15,16] In a ceramic with combined surface-compression-strengthening and weak-interface-toughening mechanisms, it is important to calculate the relaxation effect of the weak interface on the surface compressive stress accurately so the effect of the weak interface on the mechanical properties of the ceramic can be understood.

In the present study, FEM was used to calculate the thermal residual stress distribution required for optimizing the structure of a layered SiC/TiC composite and the relaxation effect of the introduction of some SiC + C weak interlayers with different compositions into the layers on the surface stress of the finally designed SiC/TiC composite. After these ceramics were fabricated, their

surface stress conditions were tested with an x-ray stress analyzer. The calculated and tested surface stresses were compared.

II. LAYERED STRUCTURE DESIGN AND FEM CALCULATIONS

A SiC/TiC composite was selected for the present work because few studies have been done on this type of layered material. The physical and elastic properties of SiC and TiC are listed in Table I. The properties of different SiC + TiC composites can be calculated according to the rule of mixtures.[17]

A 2-dimensional initial model for FEM calculation is shown in Fig. 1. The surface layer of the model is SiC, and the inner layer is TiC; the TiC layer is twice as thick as the SiC layer. In view of the symmetry, one-quarter of the model was used for calculation. The right and upper surfaces are free surfaces. All corners were pinned to prevent rigid body translations. The model was assumed to cool from 1850 to 20 °C, with a uniform temperature field. A generalized plane-stress condition was assumed, in which the strain along the Z direction was assumed constant. FEM software (MARC 7.1, MARC Analysis Research Corp., Palo Alto, CA) was used for calculation.

Figure 2 shows the thermal residual stress in the X direction, the σ_{xx} distribution, for one-quarter of Fig. 1. After the ceramic was cooled from the assumed sintering temperature, a large compressive residual stress was introduced to the surface SiC layer, but the tensile stress in the inner TiC layer was 1350 MPa, far higher than the fracture strength of TiC material.

To decrease the inner tensile stress, the thickness of the inner layer should be increased or the CTE mismatch between the surface and the inner layer decreased. To form a gradually varying stress from the surface to the inner layer, SiC + TiC layers of different compositions should be inserted between the selected surface and the inner layer. The sintered properties of the SiC/TiC composite also should be considered. Jiang *et al.* have reported that the mechanical properties of a SiC/TiC composite decrease when the TiC content exceeds 20 wt%.[18]

After several steps, a final symmetrical SiC/S10T structure was chosen for the present study, as shown in Fig. 3. The thickness ratio of SiC:S2T:S4T:S6T:S8T:S10T is 1:1:1:1:1:10. The structure modeled in Fig. 3 has the proper surface compressive stress and inner tensile stress. The σ_{xx} distribution of the model is shown in Fig. 4. On the central line of the structure (from point A to B in Fig. 4), the stress varies gradually from compressive to tensile, as shown in Fig. 5.

To introduce different weak interfacial bonding, four different SiC + C interlayers composed of 50 wt% SiC + 50 wt% C; 40 wt% SiC + 60 wt% C; 30 wt% SiC + 70 wt% C; and 20 wt% SiC + 80 wt% C were inserted into the interfaces between the different layers shown in Fig. 3. This procedure is modeled in Fig. 6. Because the thickness of the interlayers was much smaller than that of the layers,[10,11,19] the interlayer was treated as though it had zero thickness for FEM calculations. The interlayer was different from the layers in elastic property. Table II lists the elastic modulus of the SiC + C interlayers calculated from the rule of mixtures.[17] Different interlayers can be regarded as elastic springs with different elastic moduli connecting original same nodes in the FEM meshes (Fig. 6, step 3). After re-lamination, the model

TABLE I. Physical and mechanical properties of SiC and TiC.

	Elastic modulus (GPa)	Coefficient of thermal expansion (10^{-6}/K)	Density (g/cm^3)	Poisson's ratio
SiC	430	4.8	3.17	0.14
TiC	430	7.4	4.94	0.19

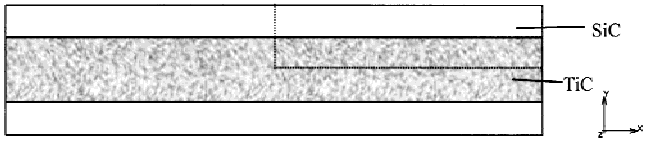

FIG. 1. Initial SiC/TiC model composite for FEM calculation.

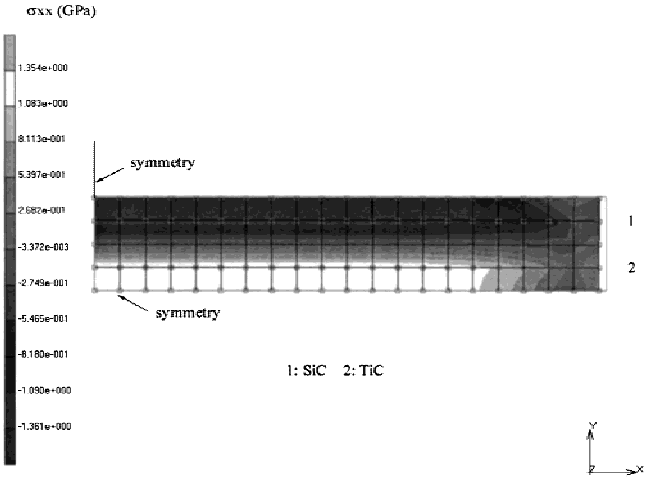

FIG. 2. σ_{xx} distribution of one-quarter of the initial SiC/TiC model.

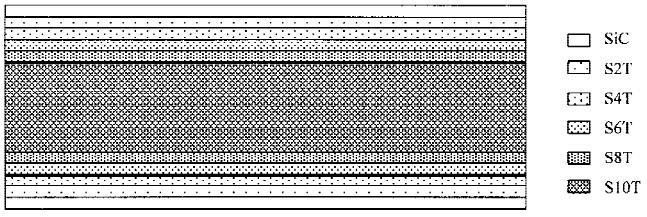

FIG. 3. Model of the finally chosen layered SiC/S10T structure (where S2T is SiC + 2 wt% TiC, S4T is SiC + 4 wt% TiC, and so forth).

was geometrically continuous but mechanically discontinuous from one layer to the adjacent layer. Then the original thermal residual stress was relaxed by the elastic springs. The original and relaxed thermal residual stress distributions from point A to B in Fig. 4 are shown in Fig. 7. It can be seen that the introduction of the weak interlayer had little relaxation effect on the residual stress distribution, and the effect is particularly small in the inner S10T layer.

III. MATERIALS AND EXPERIMENTS

Various amounts of SiC powder (0.6-μm nominal size, Norton AS Corp., Arendel, Norway) and TiC powder (3-μm nominal size, Zhuzhou Hard Alloy Factory, Zhuzhou, People's Republic of China) were mixed in deionized water with 4.8 wt% alumina (0.48-μm nominal size, Shanghai Wusong Chemical Factory, Shanghai, People's Republic of China) and 3.6 wt% yttria (4-μm nominal size, Shanghai Yuelong Chemical Factory, Shanghai, People's Republic of China) used as sintering aids. The total volume fraction of the ceramic powders in the slurry was approximately 50%. A 10% solution of tetramethylammonium hydroxide was used as the dispersant. The mixture was ball-milled for 24 h. Solutions of 10% polyvinyl alcohol (PVA) and glycerol then were added to the slurry as binder and plasticizer, respectively. After the slurry was ball-milled again for 24 h, it was degassed, using a vacuum pump, then tape cast on a fixed glass plate with a moving blade at a constant speed of 5 mm/s.

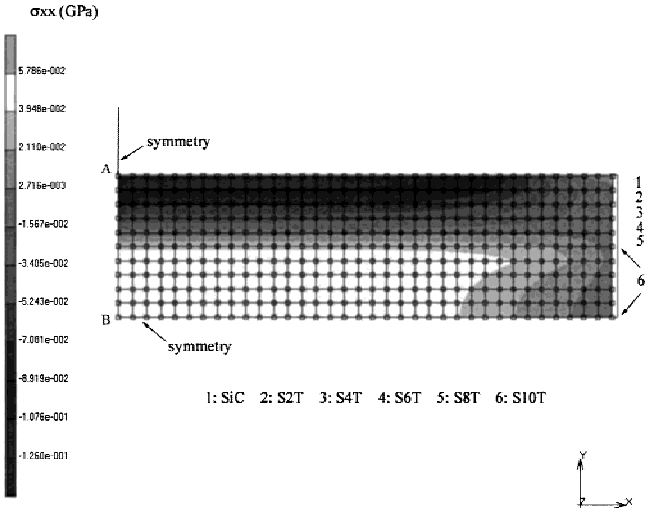

FIG. 4. σ_{xx} distribution of one-quarter of the model in Fig. 3.

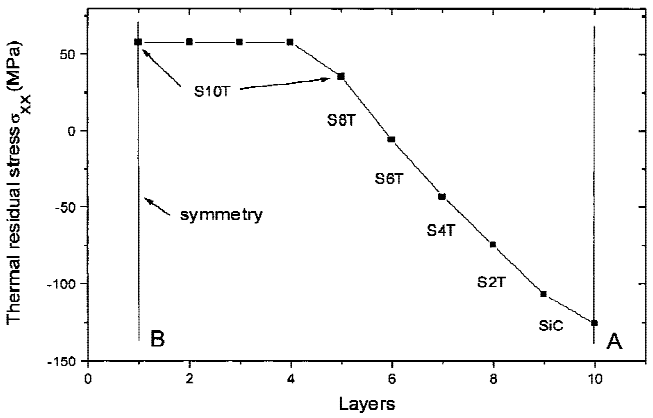

FIG. 5. σ_{xx} distribution from point A to point B in Fig. 4.

After natural drying, the green sheet was approximately 220 μm thick. The dried green sheet was cut into rectangles with dimensions of 40 mm × 50 mm. One face of different sheets was coated with SiC + C slurry. The SiC + C slurries contained 50, 60, 70, and 80 wt% graphite (9-μm nominal size, Shanghai Carbon Factory, Shanghai, People's Republic of China). Methylcellulose (MC) was used as the dispersant for graphite powder in the SiC + C slurries. The thickness of the coated SiC + C interlayer was approximately 30 μm after natural drying. Then the sheets were stacked according to the sequence in Fig. 3 to form five green ceramics, one without an interlayer and the others with 50 wt% C, 60 wt% C, 70 wt% C, and 80 wt% C interlayers. The stacked sheets were put into a graphite die for pyrolysis of the organic components at 700 °C and then hot-press sintered in argon atmosphere at 1850 °C under 35 MPa for 30 min. The sintered materials were approximately 4 mm thick.

The ceramics then were cut into nominal 3 × 4 × 40 mm (width × thickness × length) specimens. The surfaces of all of the specimens were ground carefully on a glass plate, using 32-μm and then 0.6-μm SiC powder. This process must ensure that the thickness of the surface SiC layer was the same as that of the SiC + TiC layers (except S10T). One side face of the ceramics was polished and observed by optical microscopy.

The stress conditions for the center of the surfaces of the layered SiC/S10T composites and a layered pure SiC fabricated by the same processes, which was selected as the standard sample, were tested with an x-ray stress analyzer (Model X-350A, Handan X-ray Institute, Handan, People's Republic of China). The x-ray diffraction method for measuring strains and stresses in crystalline solids has been well established.[21] In past years, many studies on measurements of residual stress and strain in ceramic matrix composites by x-ray diffraction were done.[22–25] The method essentially uses the crystal lattice as an absolute strain gauge.

When an external load is applied to a crystal the lattice distorts and d changes. By comparing the measured d value in a distorted crystal with the strain free interplanar spacing d_0, the elastic strain (ϵ) can be determined

$$\epsilon = \frac{d - d_0}{d_0} = \cot\theta_0 \frac{\Delta(2\theta)}{2} \quad ,$$

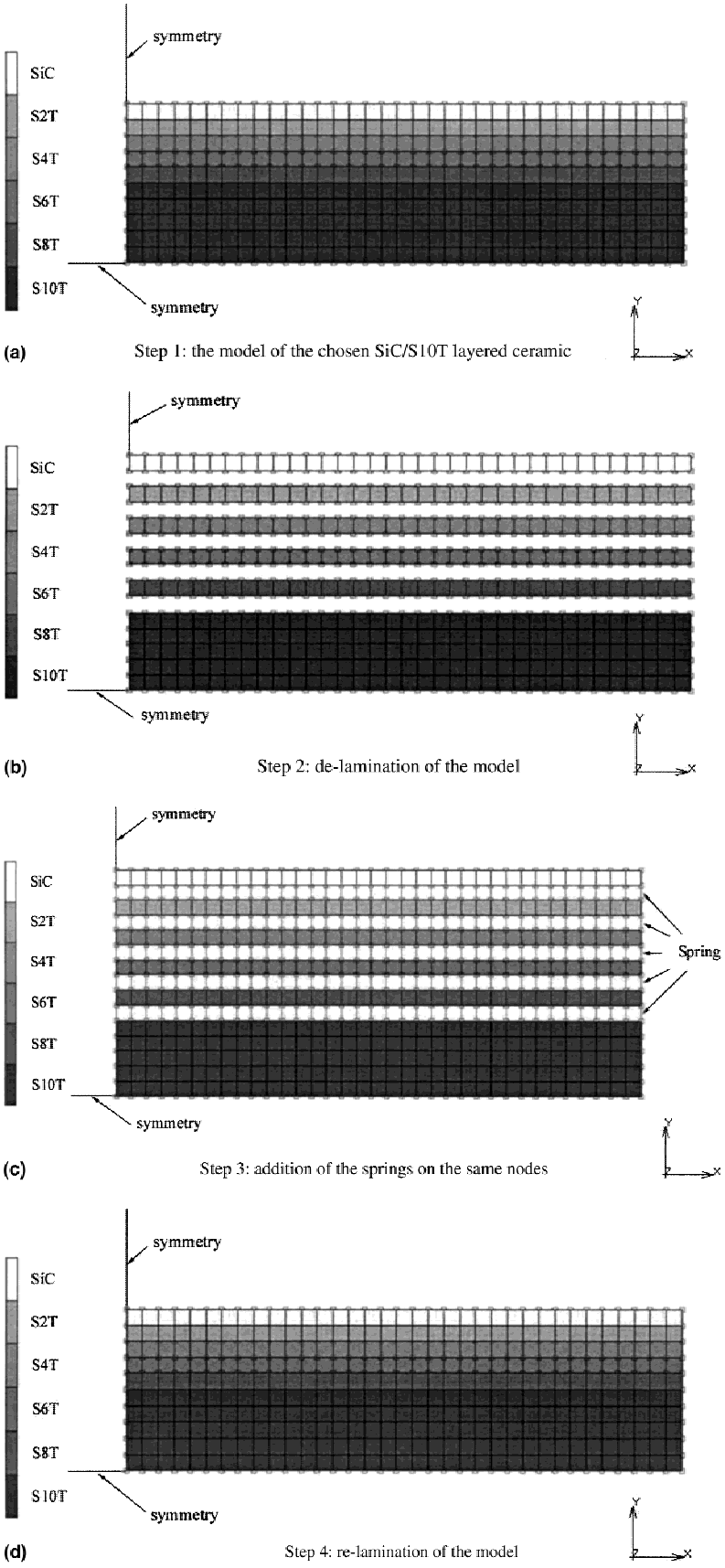

FIG. 6. Procedure of inserting the SiC + C interlayer into the interfaces between the layers.

TABLE II. Elastic modulus of the SiC + C interlayers.

Materials	Elastic modulus (GPa)
SiC	430
SiC + 50 wt%C	182
SiC + 60 wt%C	143
SiC + 70 wt%C	106
SiC + 80 wt%C	72
C[20]	10

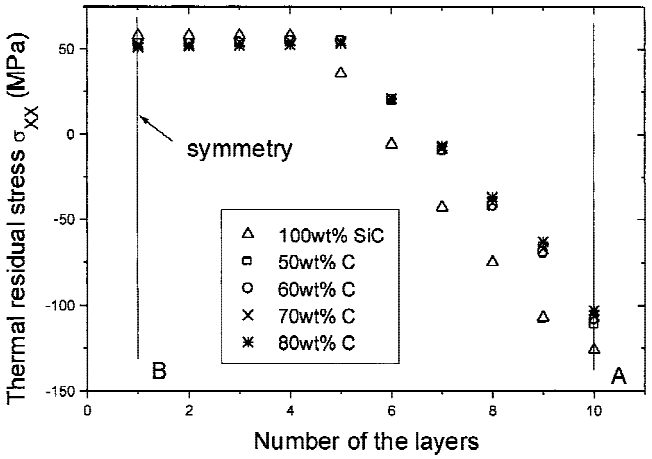

FIG. 7. Relaxation effects of the SiC + C interlayers on the σ_{xx} distribution from point A to B in Fig. 4.

where 2θ is the angle between the incident and diffracted beams, and λ is the incident wavelength. From the elastic strain, the corresponding stress can be calculated with the aid of elastic constants appropriate for the *hkl* plane used.

In this work, Cr K_α radiation was used as the x-ray source. The penetration depth of the x-ray was less than 10 μm. The (222) plane of SiC was selected as the diffraction crystal face. Biaxial stress on the surface of the specimens was assumed, and the stress along the length direction of the specimens was tested. The widely recognized $\sin^2\psi$ method was used, and measurements were made at two ψ values of 0° and 45°, corresponding to $\sin^2\psi$ values of 0 and 0.5. First, the surface stress of the layered pure SiC ceramic was tested as a standard stress. Then the surface stresses of the five layered SiC/S10T ceramics were tested. The tested stress of each layered SiC/S10T ceramic minus the standard stress was regarded as the surface thermal residual stress of the layered SiC/S10T ceramic.

IV. RESULTS AND DISCUSSION

Figure 8 shows the optical microstructures of the side faces of the five ceramics. After sintering, the interfaces between the different SiC + TiC layers in the layered SiC/S10T ceramic without interlayer disappeared completely [Fig. 8(a)]. The light phase in Figs. 8(c), 8(e), 8(g), and 8(i) is TiC particles. It can be seen that the thickness of the SiC + C interlayer increases with increasing graphite content because graphite is very difficult to sinter at this sintering temperature. The interlayers are thin, straight, and uniform. Their thickness is about 10–16 μm, which is 1/20–2/25 of the SiC + TiC layers (except S10T).

Figure 9 shows the comparison between the stresses at the center of the surface calculated by FEM and tested by x-ray diffraction. In the SiC/S10T ceramic without interlayer, the calculated surface stress, −126 MPa, is very close to the tested, −129 MPa. However, with increasing graphite content in the interlayers, the decreasing rate in the tested surface stress is faster than that in the calculated surface stress.

In the calculation of elastic modulus of the interlayer according to the rule of mixtures, the interlayer was assumed to be completely dense after sintering. However, graphite is very difficult to sinter at this temperature, so that the interlayers are porous [Figs. 8(c), 8(e), 8(g), and 8(i)]. So the elastic moduli of the interlayers used for FEM calculation are higher than that in sintered materials. Thus, the real relaxation effect of the interlayers on the surface stress is larger than that for the calculated results.

V. CONCLUSIONS

A symmetrically layered SiC/S10T ceramic with proper gradual thermal residual stress was designed by FEM. It was found that, when different SiC + C interlayers containing 50 wt% C, 60 wt% C, 70 wt% C, and 80 wt% C were introduced into the layers to weaken the interface, the interlayer had little relaxation effect on the residual stress distribution of the designed SiC/S10T ceramic by means of FEM calculation. These ceramics were then fabricated by aqueous tape casting, stacking, and hot-press sintering in argon atmosphere at 1850 °C under 35 MPa for 30 min. After sintering, the interfaces between the different layers in the layered SiC/S10T ceramic without interlayer disappeared completely. The interlayers were thin, straight, and uniform. Their thickness was about 1/20–2/25 of the SiC + TiC layers (except S10T). The surface stress conditions of the ceramics were tested by x-ray stress analysis. The tested surface stress of the layered SiC/S10T ceramic without interlayer was very close to FEM calculation. However, the real relaxation effect of the SiC + C interlayer on the surface compressive stress was much larger than the theoretical results. The reason is that the interlayer was assumed to be completely dense in the FEM model, but the real interlayer in the sintered materials was porous, so the selected elastic modulus of the interlayer for FEM calculation was higher than the real elastic modulus.

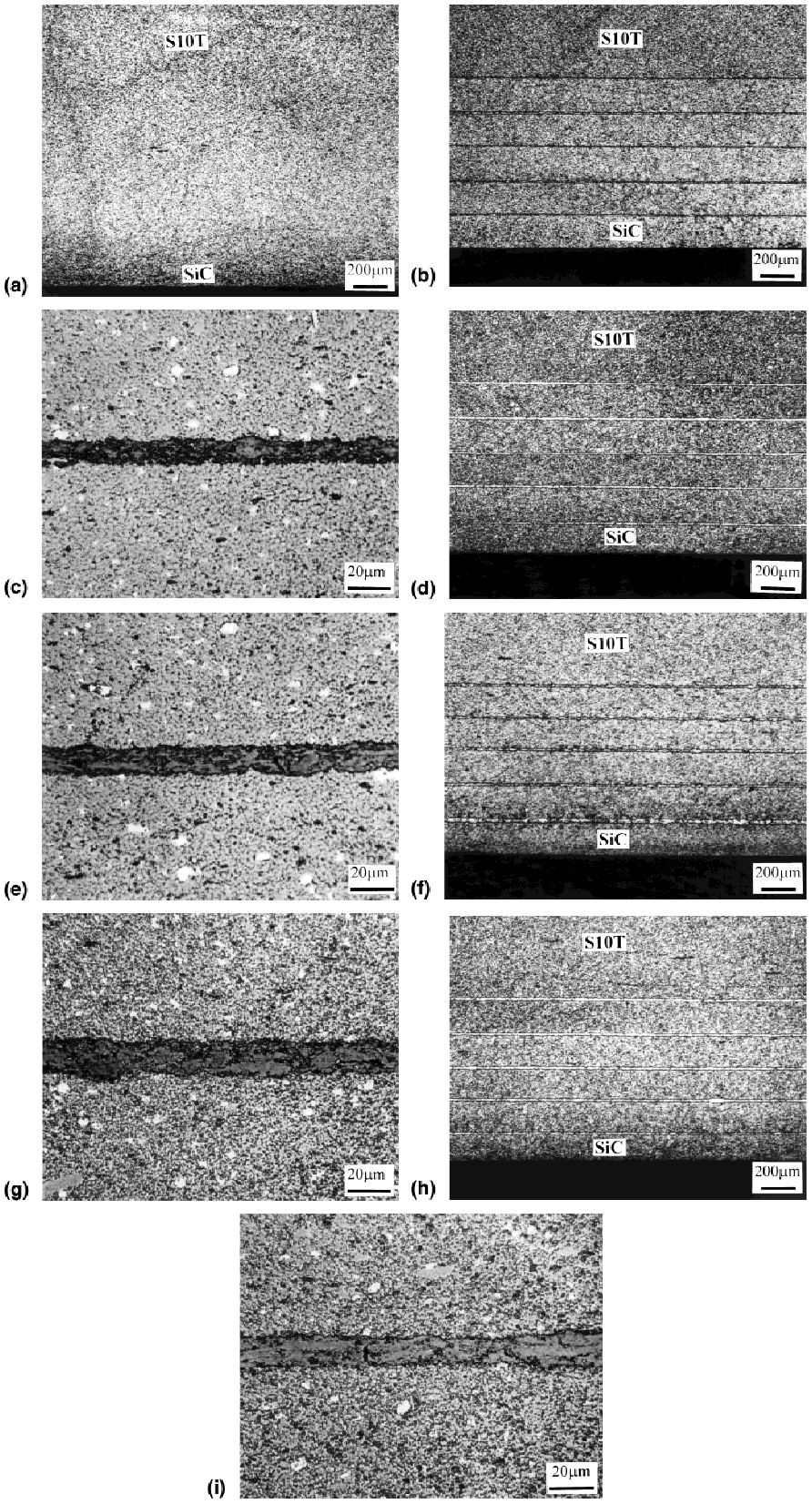

FIG. 8. Optical microstructures of the five SiC/S10T layered ceramics (a) without interlayer; (b) 50 wt% C interlayer; (c) high magnification of (b); (d) 60 wt% C interlayer; (e) high magnification of (d); (f) 70 wt% C interlayer; (g) high magnification of (f); (h) 80 wt% C interlayer; (i) high magnification of (h).

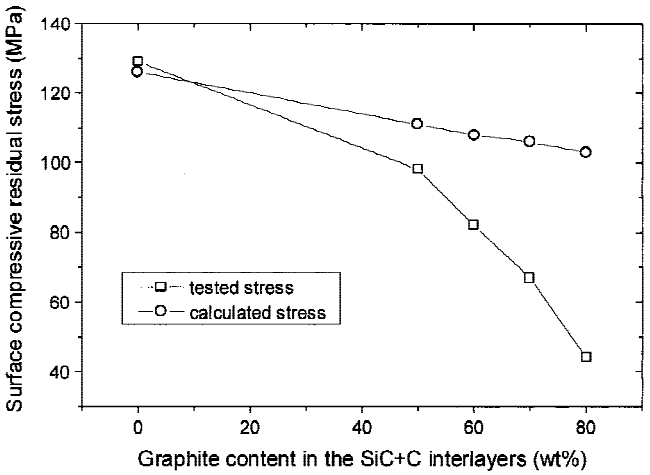

FIG. 9. Comparison between the tested and calculated surface compressive stresses.

ACKNOWLEDGMENTS

This work was financially supported by The State Key Laboratory of High Performance Ceramics and Superfine Microstructure, Shanghai Institute of Ceramics, and the Wang Kuan Cheng Post-Doc Science Foundation of the Chinese Academy of Sciences. The authors also are grateful for the support of State Key Laboratory of Metal Matrix Composites and the assistance with x-ray stress analysis by Dr. Chuanhai Jiang of the Department of Materials Science, Shanghai Jiao Tong University.

REFERENCES

1. Lakshminarayanan, D.K. Shetty, and R.A. Cutler, J. Am. Ceram. Soc. **79,** 79 (1996).
2. C.H. Yeh and M.H. Hon, Ceram. Int. **23,** 361 (1997).
3. G.J. Zhang, X.M. Yue, and T. Watanabe, J. Eur. Ceram. Soc. **19,** 2111 (1999).
4. M.P. Rao, A.J. Sanchez-Herencia, G.E. Beltz, R.M. McMeeking, and F.F. Lange, Science **286,** 102 (1999).
5. R. Sathyamoorthy, A.V. Virkar, and R.A. Cutler, J. Am. Ceram. Soc. **75,** 1136 (1992).
6. H. Wang and X.Z. Hu, J. Am. Ceram. Soc. **79,** 553 (1996).
7. A.J. Sanchez-Herencia, C. Pascual, J. He, and F.F. Lange, J. Am. Ceram. Soc. **82,** 1512 (1999).
8. S. Ho, C. Hillman, F.F. Lange, and Z. Suo, J. Am. Ceram. Soc. **78,** 2353 (1995).
9. W.J. Clegg, K. Kendall, N.McN. Alford, T.W. Button, and J.D. Birchall, Nature (London) **347,** 455 (1990).
10. W.J. Clegg, Acta Metall. Mater. **40,** 3085 (1992).
11. D. Kovar, M.D. Thouless, and J.W. Halloran, J. Am. Ceram. Soc. **81,** 1004 (1998).
12. S. Timoshenko, *Strength of Materials Part I: Elementary*, 3rd ed. (Van Nostrand Reinhold Company, New York, 1955), p. 94.
13. S.Y. Qin, C.R. Chen, G.D. Zhang, W.L. Wang, and Z.G. Wang, Mater. Sci. Eng. **A272,** 363 (1999).
14. C.R. Chen, S.X. Li, and Q. Zhang, Mater. Sci. Eng. **A272,** 398 (1999).
15. V.Q. Bui, E. Marechal, and H. Nguyen-Dang, Comp. Sci. Tech. **59,** 2269 (1999).
16. V.Q. Bui, E. Marechal, and H. Nguyen-Dang, Comp. Sci. Tech. **60,** 131 (2000).
17. W.D. Kingery, *Introduction to Ceramics* (John Wiley & Sons, New York, 1960), p. 479.
18. D.L. Jiang, J.H. Wang, Y.L. Li, and L.T. Ma, Mater. Sci. Eng. **A109,** 401 (1989).
19. E.J. Winn and I.W. Chen, J. Am. Ceram. Soc. **83,** 3222 (2000).
20. C.L. Mantell, *Carbon and Graphite Handbook* (Interscience Publishers, New York, 1968), pp. 24–25.
21. I.C. Noyan and J.B. Cohen, *Residual Stress: Measurement by Diffraction and Interpretation* (Springer-Verlag, New York, 1987), pp. 117–162.
22. P. Predecki, A. Abuhasan, and C.S. Barrett, Adv. X-Ray Anal. **31,** 231 (1988).
23. R.M. Fullrath, J. Am. Ceram. Soc. **42,** 423 (1959).
24. A. Abuhasan, C. Balasingh, and P. Predecki, J. Am. Ceram. Soc. **73,** 2474 (1990).
25. L.N. Grossman and R.M. Fullrath, J. Am. Ceram. Soc. **44,** 567 (1961).